Applied Surface Science 292 (2014) 197–203

Contents lists available at ScienceDirect

Applied Surface Science

journal homepage: www.elsevier.com/locate/apsusc

Deformation-phase transformation coupling mechanism of white layer formation in high speed machining of FGH95 Ni-based superalloy

Jin Du[a], zhanqiang Liu[b,c,*], Shaoyu Lv[b]

[a] School of Mechanical & Automotive Engineering, Qilu University of Technology, Jinan, Shandong 250353, China
[b] School of Mechanical Engineering, Shandong University, Jinan, Shandong 250061, China
[c] Key Laboratory of High Efficiency and Clean Mechanical Manufacture, Shandong University, Ministry of Education, Shandong, China

ARTICLE INFO

Article history:
Received 21 August 2013
Received in revised form
20 November 2013
Accepted 20 November 2013
Available online 28 November 2013

Keywords:
White layer
FGH95
High speed machining
FEM

ABSTRACT

Ni-based superalloy represents a significant metal portion of the aircraft critical structural and engine components. When these critical structural components in aerospace industry are manufactured with the objective to reach high reliability levels and excellent service performance, surface integrity is one of the most relevant parameter used for evaluating the quality of finish machined surfaces. In the study of surface integrity, the formation white layer is a very important research topic. The formation of white layer on the Ni-based superalloy machined surface will reduce the machined parts service performance and fatigue life. This paper was conducted to determine the effects of cutting speed on white layer formation in high speed machining of FGH95 Ni-based superalloy. Optical microscope, scanning electron microscope and X-ray diffraction were employed to analyze the elements and microstructures of white layer and bulk materials. The statistical analysis for grain numbers was executed to study the influence of cutting speed on the grain refinement in the machined surface. The investigation results showed that white layer exhibits significantly different microstructures with the bulk materials. It shows densification, no obvious structural features characteristic. The microstructure and phase of Ni-based solid solution changed during cutting process. The increase of cutting speed causes the increase of white layer thickness when the cutting speed is less than 2000 m/min. However, white layer thickness reduces with the cutting speed further increase. The higher the cutting speed, the more serious grains refinement in machined surface. 2-D FEM for machining FGH95 were carried out to simulate the cutting process and obtained the cutting temperature field, cutting strain field and strain rate field. The impact mechanisms of cutting temperature, cutting strain and strain rates on white layer formation were analyzed. At last, deformation-phase transformation coupling mechanism was proposed to illustrate the white layer formation mechanism in high speed machining of PM superalloy.

1. Introduction

Ni-based superalloys have the ability to retain most of their strength even after long exposures to extremely high temperatures and are the only material of choice for turbine sections of the jet engines. The main strengths of the Ni-based superalloys are being heat-resistant, retaining their high mechanical and chemical properties at high temperatures, and having high melting temperatures, high corrosion resistance, as well as resistance to thermal fatigue, thermal shock, creep, and erosion [1–3]. FGH95 Ni-based superalloy is a powder metallurgy (PM) superalloy and often used in the hot sections of mission critical components in jet engines or gas turbine engines. Although FGH95 superalloy is formed by powder metallurgy process which can produce near net shape parts, finishing are till needed to meet tolerance requirements or better surface integrity. In the finish machining, surface integrity of FGH95 superalloy is often of great concern because of their impact on product performance in terms of functional behavior and dimensional stability. However, PM Ni-based FGH95 superalloy is extremely difficult to machine due to its several inherent properties, including lowing of thermal conductivity that leads to elevating temperatures at the tool/chip interface during cutting, work hardening tendency during machining that becomes more severe with increased strengthening of this superalloy, and intensive adhesion to the surface of the tooling under operation [4–7]. These properties are likely to increase temperature and stresses on the tool face, degrade the integrity of finished surface and cause tool damages such as flank wear, notching wear, edge chipping

* Corresponding author. Tel.: +86 158 53120838; fax: +86 531 88393206.
E-mail address: melius@sdu.edu.cn (z. Liu).

0169-4332/$ – see front matter © 2013 Elsevier B.V. All rights reserved.
http://dx.doi.org/10.1016/j.apsusc.2013.11.111

etc., resulting in short tool life [8]. In the machining of Ni-based superalloy, machined surface microstructure will lead to change and, consequently, to the mechanical properties and quality of the surface. Typically, these changes – commonly referred to as 'white layer' – are confined to a few tens micrometers into the subsurface [9]. Although the term 'white layer' has become the customary way of referring to such layers, other terms such as white etching layer, non-etching layers, white phase, phase transformed materials are also used [10]. According to Veldhuis [11], a 2–4 μm thick white layer formed on the machined surface in finishing turning operation of Ni-based PM superalloy ME16. Formation of the white layer poses a significant potential danger to fatigue life. Since the FGH95 Ni-based PM superalloy to be used in critical engine components, this issue must be resolved first.

White layer can be found in many material removal processes such as turning, reaming, grinding and electrical discharge machining [12]. It is appears white under an optical microscope or featureless in a Scanning electron microscopy (SEM), therefore called 'white layer'. The characteristics of white layers are commonly recognized as resistance to etching by conventional agents, high microhardness and increased wear resistance [13,14]. It was found to be of high hardness compared to the bulk materials and featureless when observed under an optical microscope. In particular, white layer is typically a few microns thick, and it is hard and brittle since it is known to be the result of microstructural alteration. Three key mechanisms responsible for white layer formation in various manufacturing processes are identified by Griffith [15] as (1) phase transformation due to rapid heating and quenching, termed the thermal effect; (2) fine grain structure formed due to severe plastic deformation, termed the mechanical effect; (3) reaction of the surface with the environment. With the exception of a few investigators, most of the current literature suggests or assumes that white layers formed in machining of hardened steels are due to a thermally-induced martensitic (γ–α) phase transformation effect [16–18]. Kevin [7] reports that white layer formation seems to be dominantly a rapid heating-cooling process. However, it is also believed that plastic deformation will assist grain refinement and phase transformation processed. Sangil [15] presents that white layer formation in machining of AISI 1045 annealed steel occurs at a temperature below the nominal phase transformation temperature in the Fe–C phase diagram. Plastic deformation in the machining process is thought to play a role in causing phase transformation below the nominal phase transformation temperature. Therefore, it is apparent that white layers may be formed by phenomena other than thermally-driven martensitic phase transformation. In all, two mechanisms, thermal and mechanical effects, are considered to be the major causes of white layer formation in the machining of superalloys.

Table 1
Chemical compositions of the studied FGH95 (wt%).

C	Cr	Co	W	Mo	Al	Ti	Nb	Ni
0.060	12.98	8.00	3.40	3.40	3.48	2.55	3.50	Bal

At present, there are few studies focus on the white layer formation mechanisms and its mechanical properties in the machining of PM superalloy. There is also lack of the research on the influences of cutting speed on the white layer formation in high speed machining of PM superalloy. To date there is not much information available on the white layer formation of PM superalloy FGH95. Thus, the aim of this paper is to analyze the properties and mechanisms of white layer formed on the machined surface in high speed machining of FGH95 Ni-based superalloy at different cutting speeds. It also seeks to reveal the roles of grain refinement on white layer formation in high speed machining. This is accomplished through a systematic experimental investigation involving SEM, EDS, X-ray diffraction (XRD). Finite Element Simulation is also employed to simulate the cutting temperature, cutting strain and strain rate in the machined surface during high speed machining of FGH95. The simulation results were adopt to analyze the effects of machined surface temperature, strain and strain rate on the white layer thickness and then to research the mechanism of white layer formation in high speed machining of FGH95 superalloy. This investigation can provide theoretical guidance on the investigation of machined surface white layer formation in high speed machining of FGH95 PM superalloy. It also has important significance to investigate the surface integrity of FGH95 PM superalloy, thus can improve the FGH95 parts service performance and fatigue lives.

2. Experimental

2.1. Work material and cutting tools

The workpiece materials are PM Ni-based superalloy FGH95. The chemical compositions of FGH95 are given in Table 1 [19]. The microstructures of FGH95 after HIP and normal heat treatment is exhibited in Fig. 1. From Fig. 1(a), it can be seen that grain boundaries are clearly visible, the average grain sizes is about ASTM 6–7. There exist primary particle boundaries (PPB) and thermally induced porosity (TIP) in the FGH95 bulk material. PPB particles originated from γ' phase were related to characteristics of the powder particles atomized by plasma rotating electrode process (PREP). TIP is discontinuous porosities which formed in the HIPed products after heating in the subsequent process due to the insoluble inert gas expansion. From Fig. 1(b), the grain boundaries and TIP can also be seen clearly. PPB and TIP are the crack sources that

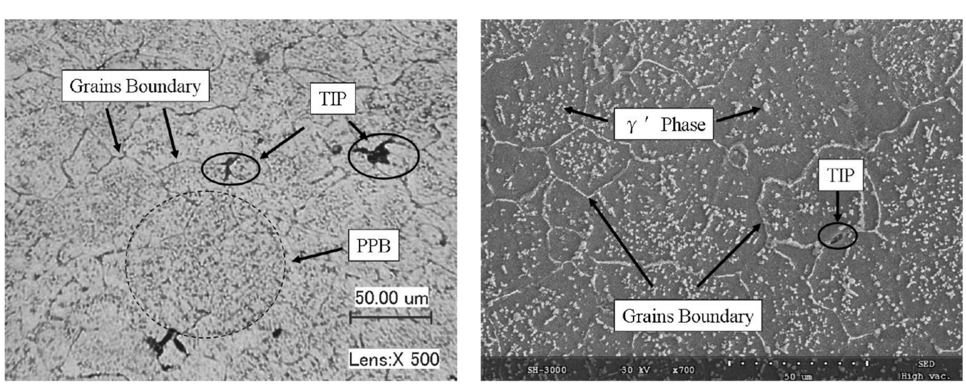

(a) Optical image (b) SEM image

Fig. 1. Microstructure of FGH95 after HIP.

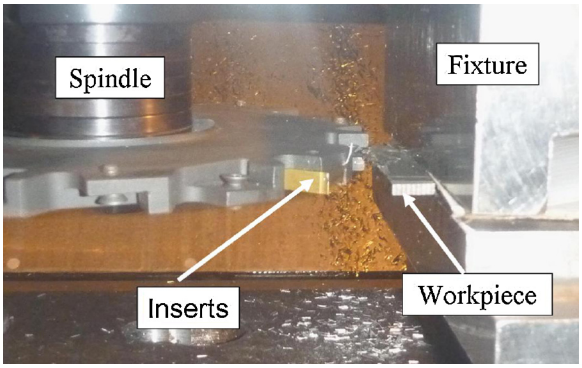

Fig. 2. Workpiece and cutting inserts employed in the experiments.

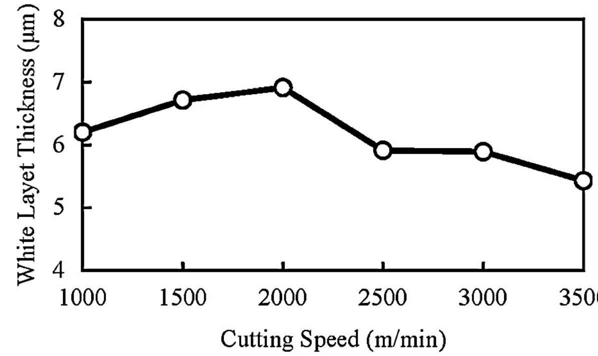

Fig. 4. Variation of white layer thickness with cutting speed.

decrease stress rupture and tensile ductility, and make the machinability of FGH95 worsen. In Fig. 1(b), γ' phase was observed. The coarse γ' precipitates exhibited irregular blocky shapes with a size greater than 1 μm, and mainly precipitated at the grain boundaries; the fine γ' precipitates were nearly spherical, they are dispersed precipitation in the grains.

2.2. Machine tool

The cutting experiments were carried out on a 3-axis CNC machining center with maximum spindle rotation speed 10,000 rpm. The FGH95 superalloy was cut-off into sheet specimens in order to mounting in the special fixture as shown in Fig. 2. The cutting tool employed in this experiment was face milling cutter supplied by KENNAMETAL INC. The cutting inserts geometry applied in this experiment are SNHX12L5PZTNGP KC725 M with TiN, AlTiN advanced PVD coatings. Before each experimental cutting, the inserts were changed to a fresh one in order to eliminate the influence of tools wear on the machined surface integrity. In this study, the effects of cutting speed on the white layer formation in high speed machining of FGH95 were investigated. The cutting speeds employed in this experiment were 1000, 1500, 2000, 2500, 3000 and 3500 m/min. The axial depth of cut was maintained constant at 2.5 mm and feed was maintained constant at 0.01 mm/r, respectively. The cutting tests were all dry cutting condition.

3. Experimental results and discussion

3.1. Microstructure changes

After each test cutting, workpiece sections measuring 10 mm × 10 mm were cut out from the machined surface using EDM in order to mount in the Bakelite. Then, the samples were polished and etched with 2.5% copper chloride, 48.8% hydrochloric acid, and 48.7% ethanol to check for the white layer and its depth. The metallographic samples of machined workpieces were etched using copper sulfate solution, and then observed under optical microscope and SEM. The optical and SEM images of FGH95 machined surface white layer are shown in Fig. 3. It can be seen from Fig. 3(a) that microstructures and grains in the FGH95 superalloy bulk are clearly visible, but at the machined surface or subsurface they showing a different structure characteristics. On the machined surface covered a thin layer, this layer shows bright white under the optical microscope, it is white layer. From Fig. 3(a), a dark region appears beneath the white layer, called "transition region" or "dark layer" [20]. The microstructure of white layer under the SEM is shown in Fig. 3(b), this layer exhibits significantly different microstructures with the bulk materials. It shows densification, no obvious structural features characteristic. Beneath the white layer, the dark layer shows strong plastic flow characteristic along the cutting direction. It proves that the material plastic flow occurred along the cutting direction in the cutting process. Followed by dark layer, strengthen phase γ′ can be clearly displayed and evenly distributed in FGH95 bulk material.

The influence of cutting speed on the white layer thickness is exhibited in Fig. 4. It can be seen from Fig. 4 that the increase of cutting speed causes the increase of white layer thickness when the cutting speed is less than 2000 m/min. However, white layer thickness reduces with the cutting speed further increase when other cutting parameters remain the same. The maximum thickness of white layer is obtained at the cutting speed of 2000 m/min. At this cutting speed, the maximum thickness of white layer is 6.91 μm.

3.2. EDS analysis for white layer

EDS analysis can be applied to material composition and micro elements analysis. It can be used to semi-quantitative elements

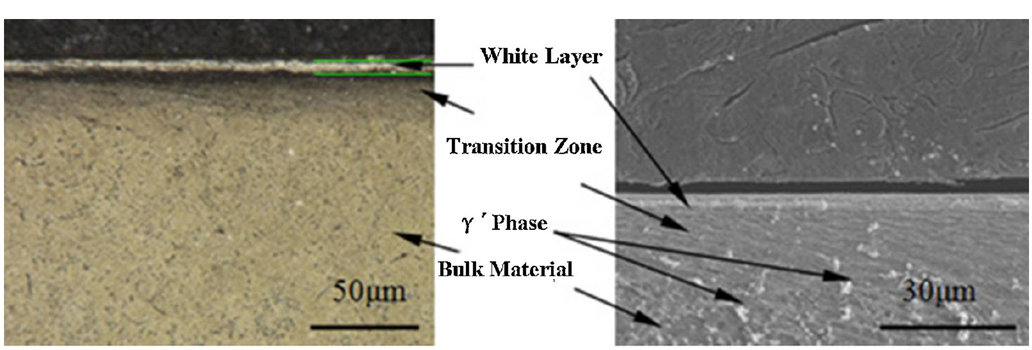

(a) Optical image (b) SEM image

Fig. 3. White layer formed at cutting speed of 1000 m/min.

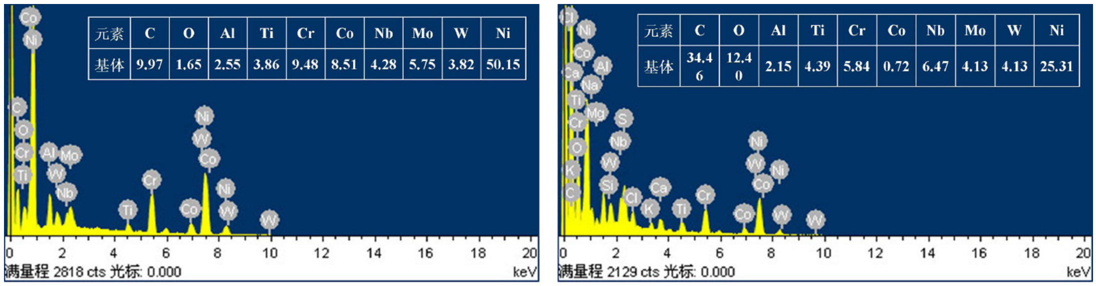

(a) Bulk materials (b) Whiter layer

Fig. 5. EDS analysis for bulk materials and white layer.

analysis. EDS analysis for white layer and bulk materials of FGH95 are listed in Fig. 5. The elements contents contrast between white layer and bulk materials can be clearly seen that the elements Ti, Nb contents in white layer increases, while the elements Cr, Co contents to reduce. It can be inferred that the strengthening phase γ' content increases by 8–15% according to the elements Ti, Nb are mainly into strengthening phase γ' while the elements Cr, Co are mainly into bulk phase γ. It can be drawn that happened a strengthening phase γ' precipitate dispersion during machining. In addition, the elements C and O contents increase more obviously in white layer, it can be drawn that the oxides and carbides content increase in white layer.

3.3. White layer phase analysis

X-ray diffraction (XRD) can be used to phase qualitative analysis of materials, grain size and lattice distortion measurement and the determination of crystallinity. In this investigation, XRD is applied to phase qualitative analysis and strengthening phase particle size measurement. XRD diffraction spectrum for FGH95 bulk material and white layer is shown in Fig. 6. From Fig. 6, it can be seen that XRD spectrum for white layer is exhibited lower and wider lines than for bulk material. This shows that white layer has poor crystallinity than bulk material and grains refinement is appeared in white layer. Post-processing for XRD spectrum can be drawn that the crystallinity of white layer is 41.38, the crystallinity of bulk material is 63.93. Through the XRD phase analysis for FGH95 bulk material and white layer show that the FGH95 alloy bulk materials is existed as the form of Ni-based solid solution. The solutes of Ni-based solid solution in FGH95 bulk materials are element Al, Cr, W, Ta, Nb, Mo, Co, and others, and the retrieved phases have a high matching with XRD PDF cards. The XRD phase analysis results for FGH95 white layer show that the white layer is also existed as the form of Ni-based solid solution, the solutes are also element Al, Cr, W, Ta, Nb, Mo, Co, and others. From the XRD phase analysis, it can also be drawn that Ni-based solid solution of FGH95 alloy occurred phase transformation during cutting process.

3.4. Grain refinements in white layer

Metallographic observation was used to observe and record the FGH95 bulk materials and machined surface microstructure images obtained at various cutting speeds. Then IPP software was employed to deal with the metallographic pictures, outline the grain boundaries at the area of 227 μm $\times$ 174 μm, measure the grains equivalent diameter and count the numbers of grain. The influence of cutting speed on grain numbers at the area of 227 μm $\times$ 174 μm is shown in Fig. 7.

It can be seen from Fig. 7 that grain numbers within the sampling area increase with the increasing of cutting speed. This is a reflection of the phenomenon of grain refinements, and the higher cutting speed, the more serious grain refinements. This indicates that the large grains and medium grains occurs dynamic recrystallization during the cutting process. This is due to the cutting will lead to the generation of dislocations within the FGH95 superalloy. With the increasing of cutting speed, more dislocations were generated in FGH95 material. Excessive dislocations can not be offset, resulting the increasing of recrystallized grain nucleation. Thus, grain refinements phenomenon is more serious. In addition, the original grains can be broken by shear and compression in cutting process, thus smaller grains can be obtained.

4. FEM simulation for the machining of FGH95

Advantedge^{TM} metal cutting simulation software was employed to simulate the cutting process of FGH95. In this paper, power law

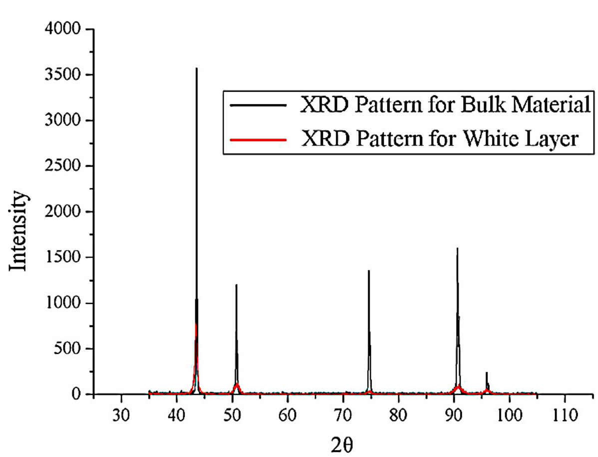

Fig. 6. XRD patterns for bulk materials and white layer.

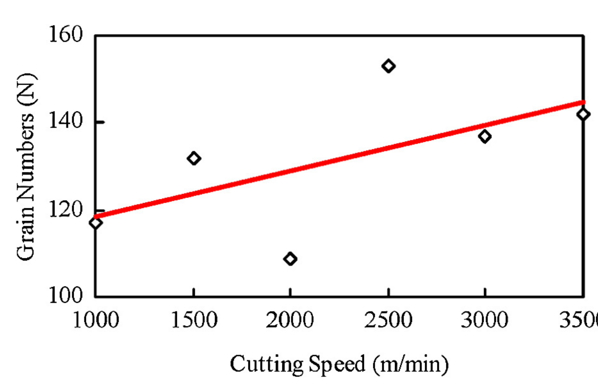

Fig. 7. Influence of cutting speed on grain numbers.

Table 2
Simulation parameters.

Workpiece parameters	Tools parameters	Cutting parameters	Lubricating
Length: 3.0 mm	Rake angle: 5°	Depth of cut: 0.02 mm	Dry cutting
Height: 1.0 mm	Flank angle: 10°	Length of cut: 2 mm	
Material: FGH95	Cutting edge radius: 0.02 mm	Feed: 0.01 mm/r	
	Tools material: TiAlN coated carbide	Cutting speed: 1000, 1500, 2000, 2500, 3000, 3500 m/min	

model was proposed to represent the plasticity behavior of FGH95. Its constitutive model is as follows:

$$\sigma(\varepsilon^p, \dot{\varepsilon}, T) = G(\varepsilon^p) * \Gamma(\dot{\varepsilon}) * \Theta(T) \quad (1)$$

where, $G(\varepsilon^p)$ is the strain hardening coefficient, $\Gamma(\dot{\varepsilon})$ is the strain rate coefficient, $\Theta(T)$ is the temperature softening coefficient.

Input parameters for FEM modeling are same as the actual machining parameters, as shown in Table 2.

In simulation model, the adaptive grid technology was applied. Assumed that workpiece was fixed, the displacement constraints was set on the both sides and the bottom of workpiece to limit the displacement of the workpiece in the *X* and *Y* directions. The initial temperature in the simulation was set to 20 °C.

5. Simulation results

After the FEM simulation, the machined surface temperature, strain and strain rate was analyzed to study the mechanism of white layer formation. The temperature, strain and strain rate at different depth in the machined surface were recorded to analyze the effects of cutting temperature and plastic deformation on white layer thickness. In this study, three regions (white layer region, boundary and non-white layer region) were selected to analyze the distribution of cutting temperature, strain and strain rate in machined surface then to illustrate the mechanism of white layer formation in high speed machining of FGH95 superalloy.

Fig. 8 presents the temperature distribution on the white layer boundary and adjacent subsurface at different cutting speed in the FGH95 Ni-based PM superalloy cutting simulation. From Fig. 8, it can be seen that the minimum temperature in white layer is 660 °C at cutting speed of 1000 m/min and in non-white layer region the maximum temperature is 809 °C at cutting speed 3500 m/min. This shows that white layer is not formed when the temperature reaches to 809 °C in non-white layer region. However, white layer is formed when the temperature is 660 °C in the white layer region. It can be drawn that cutting temperature is not the only decisive factor on the formation of white layer. It can also be seen from Fig. 8 that the minimum temperature of white layer formation is 660 °C, this temperature value is far less than the phase transition temperature (980–1050 °C) of FGH95. This also illustrate that the phase transition in white layer is not occurred only in the role of cutting temperature.

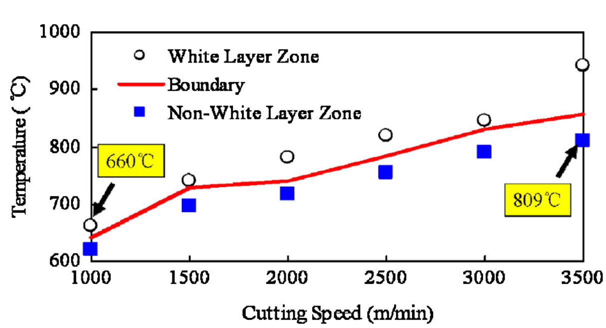

Fig. 8. Temperature distribution on the white layer boundary and adjacent subsurface.

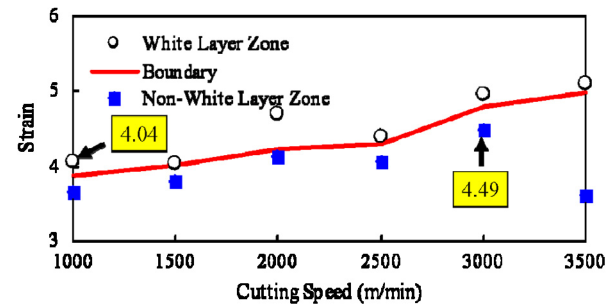

Fig. 9. Strain distribution of white layer boundary and adjacent subsurface.

The strain distribution on white layer boundary and adjacent subsurface at different cutting speed is exhibited in Fig. 9. From Fig. 9, it can be seen that the minimum strain in white layer is 4.04 and in non-white layer region the maximum strain is 4.49 at the cutting speed range of 1000–3500 m/min. This shows that white layer is not formed when the strain reaches to 4.49 in non-white layer region. However, white layer is formed when the strain is 4.04 in the white layer region. It can be drawn that strain is not the only decisive factor on the formation of white layer. Therefore, only apply the plastic deformation mechanism to reveal the white layer formation mechanism is inaccurate.

Cutting strain rate as an important component of the deformation parameters have a major impact on the dynamic properties of materials. Thus, the cutting strain rate is adopted to study the white layer formation mechanism. Fig. 10 exhibits the cutting strain rate distribution on the machined surface white layer boundary and adjacent subsurface at the different cutting speed in the cutting process simulating of FGH95. In Fig. 10, the minimum strain rate is $3.41 \times 10^5\ \mathrm{s}^{-1}$ in the white layer region, while the maximum strain rate is $1.22 \times 10^6\ \mathrm{s}^{-1}$ in the non-white layer region. Similar to the distributions of temperature and strain, white layer is not formed when the strain rate reaches to $3.41 \times 10^5\ \mathrm{s}^{-1}$ in non-white layer region, however, white layer is formed when the strain rate is $1.22 \times 10^6\ \mathrm{s}^{-1}$ in the white layer region. It can be drawn that strain rate is not the only decisive factor on the formation of white layer.

From Figs. 8–10, it can be seen that cutting temperature, strain and strain rate are all not the only decisive factor on the white layer formation. In high speed machining of FGH95 superalloy, workpiece materials withstand severe plastic deformation, this can cause larger strain and strain rate inside the material. The large strain and strain rate can reduce the phase transformation

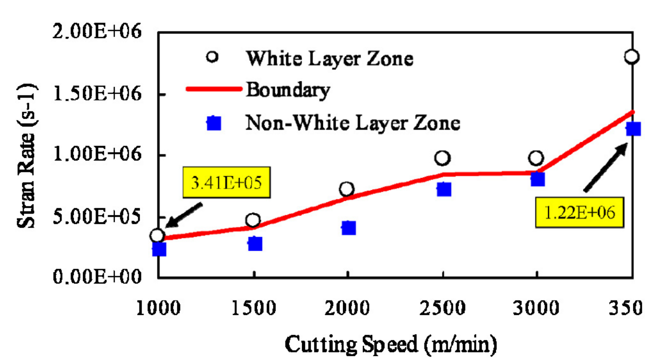

Fig. 10. Strain rate distribution on the white layer boundary and adjacent subsurface.

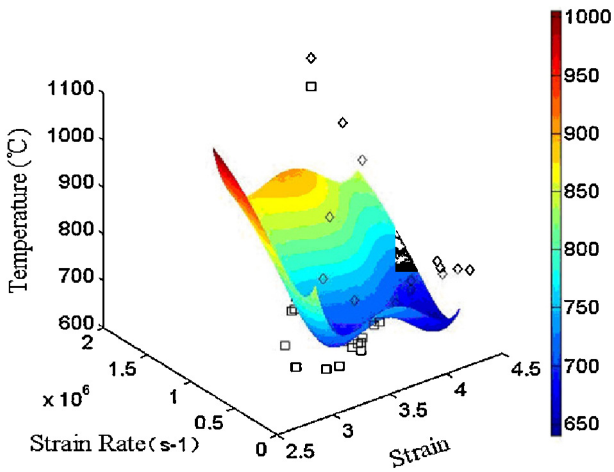

Fig. 11. Specific surface for white layer region and non-white layer region.

temperature of FGH95. Therefore, the combined effects of elevate temperature, larger strain and strain rate eventually lead to the formation of white layer in FGH95 machined surface.

Fig. 11 shows the deformation parameters distribution obtained in the cutting speed range of 1000–3500 m/min. From Fig. 11, the deformation parameters in white layer region are located above a specific surface, and the deformation parameters out of the white layer region are located under the specific surface, and the deformation parameters in the white layer boundary are located on this specific surface. In Fig. 11, the critical temperature of FGH95 machined surface white layer formation decrease as the increase of cutting strain. This illustrates that the plastic deformation of materials can induce the decrease of critical temperature of white layer formation, it can promote the white layer formation. This is consistent with the conclusion of Hans [21] and Dai [22]. Contrast to cutting strain, with the increasing of strain rate the critical temperature in white layer formation increased. This shows that higher strain rate can prevent the white layer formation.

Therefore, this specific surface can be applied to distinguish the region of white layer and non-white layer. It can be defined as the critical condition of white layer formation. Therefore, Fig. 11 can be employed to predict the white layer formation in high speed machining of FGH95 Ni-based PM superalloy. When the points jointly identified by the cutting temperature, strain and strain rate are located above this specific surface, white layer will form. When the points jointly identified by the cutting temperature, strain and strain rate are located under the specific surface, white layer will not form. The location of the specific surface is determined by the combined effects of temperature, strain, and strain rate. It can be drawn that the white layer formation is related to the coupling effects of cutting temperature, strain, and strain rate.

6. Deformation-phase transformation coupling mechanism of white layer formation

From the analysis of the machined surface white layer microstructure, it is can be drawn that not only grains refinement phenomenon is appeared, but also the strength phase diffusion precipitation is occurred. The lattice mismatch of matrix phase and strengthen phase are also changed, the primary particle boundary (PPB) is disappeared in white layer region. Obviously, the mechanism of white layer formation in high speed machining of superalloy is simply attributed to the phase transformation mechanism or deformation mechanism is not appropriate. Therefore, the deformation-phase transformation coupling mechanism is presented aim to clarify the mechanism of white layer formation in high speed machining of PM superalloy. “Deformation” in deformation-phase coupling mechanism is stand for the grains refinement in the machined surface white layer of PM superalloy and the “Phase transformation” is stand for the changes of matrix phase and strengthen phase in PM superalloy machined surface white layer. The mechanism can be described as follows:

1. Severe plastic deformation caused by the high cutting force creates the grains refinement in the machined surface white layer of PM superalloy.
2. The matrix phase γ and strengthen phase γ' was transformed, that is to say the diffusion precipitation of strengthen phase is appeared.
3. Cutting temperature, strain and strain rate are not the only decisive factor for white layer formation, the formation of white layer is related to the coupling of these three factors.

7. Conclusions

In this paper, the microstructure of white layer appeared on the machined surface was investigated in the high speed machining of FGH95 PM superalloy. FEM simulation was applied to illustrate the mechanism of white layer formation. A deformation-phase transformation coupling mechanisms of white layer formation was proposed. The following conclusions can be drawn from this study:

(1) White layer exhibits significantly different microstructures with the bulk materials. It shows densification, no obvious structural features characteristic. The increasing of cutting speed causes the increase of white layer thickness when the cutting speed is less than 2000 m/min. However, white layer thickness reduces with the cutting speed further increase when other cutting parameters remain the same.
(2) FGH95 superalloy bulk material exists as the form of Ni-based solid solution. The microstructure and the phase of Ni-based solid solution transformed during the cutting process. Meanwhile, the strengthening phase γ' contents in white layer increased by 8–15%.
(3) Cutting temperature, strain and strain rate are not the only decisive factor for white layer formation, the formation of white layer is related to the coupling of these three factors. Severe plastic deformation can reduce the phase transformation temperature in FGH95. The combined effects of elevate temperature, larger strain and strain rate eventually lead to the formation of white layer in FGH95 machined surface.
(4) The specific surface for deformation parameters of white layer region and non-white layer region is depicted. It can be used to the prediction of white layer formation in the machining of Ni-based PM superalloy.

Acknowledgments

This work has been supported by the National Natural Science Foundation of China (51375272 and U1201245), Mega-project of High-grade NC Machine Tools and Basic Manufacturing Equipment (2014ZX04012-014).

References

[1] Q. Wu, Serrated Chip Formation and Tool-edge Wear in High-speed Machining of Advanced Aerospace Materials, Utah State University, Logan, Utah, 2007.
[2] R.M. Saoubi, J.C. Outeiro, H. Chandrasekaran, O.W. Dilon, I.S. Jawahir, Int. J. Sustain. Manuf. 1–2 (2008) 203–236.
[3] Y.B. Guo, W. Li, I.S. Jawahir, Mach. Sci. Technol. 13 (2009) 437–470.
[4] Y.K. Chou, C.J. Evans, Int. J. Mach. Tools Manuf. 39 (1999) 1863–1881.
[5] S. Akcan, S. Shah, S.P. Moylan, P.N. Chhabra, S. Chandraseksar, H.Y. Yang, Metall. Mater. Trans. 33A (2002) 1245–1254.

[6] E. Brinksmeier, T. Brockhoff, High speed machining, in: Proceedings of Second International German and French Conference, 1999, pp. 7–13.
[7] Y.C. Kevin, J.E. Chris, Int. J. Mach. Tools Manuf. 39 (1999) 1863–1881.
[8] O. Toshiyuki, Y. Masashi, F. Kazuhiro, K. Yasuhiro, Y. Sachio, Int. J. Mach. Tools Manuf. 61 (2012) 20–26.
[9] U. Durul, O. Tugrual, Int. J. Mach. Tools Manuf. 53 (32) (2011) 250–280.
[10] S.S. Bosheh, P.T. Mativenga, Int. J. Mach. Tools Manuf. 46 (2006) 225–233.
[11] S.C. Veldhuis, G.K. Dosbaeva, A. Elfizy, G.S. Fox-Rabinovich, T. Wagg, J. Mater. Eng. Perform. 19 (7) (2010) 1031–1036.
[12] G. Poulachon, A. Albert, M. Schluraff, I.S. Jawahir, Int. J. Mach. Tools Manuf. 456 (2005) 211–218.
[13] A. Attanasio, D. Umbrello, C. Cappellini, G. Rotella, R.M. Saoubi, J. Wear 286–287 (2012) 98–107.
[14] Y.Y. Yang, H.S. Fang, W.G. Huang, Int. J. Tribol. 29 (1996) 425–428.
[15] H. Sangil, N.M. Shreyes, S.H. Michael, R.W. Thomas, Mater. Sci. Eng., A 488 (2008) 195–204.
[16] Y.H. Xu, L. Fang, Q.H. Cen, J. Wear 258 (1) (2005) 537–544.
[17] Y.B. Guo, A.W. Warren, F. Hashimoto, CIRP J. Manuf. Sci. Technol. 2 (2) (2010) 129–134.
[18] J.F. Peng, C. Song, M.X. Shen, Int. J. Tribol. 44 (11) (2011) 1417–1426.
[19] S.H. Zhang, B.F. Hu, H.Y. Li, C.J. Jin, K.S. Wu., J. Univ. Sci. Technol. Beijing 1 (1993) 1–9.
[20] Y.H. Xu, L. Fang, Q.H. Cen, J.H. Zhu, J. Wear 258 (2005) 537–544.
[21] S. Han, S.N. Melkote, M.S. Haluska, Mater. Sci. Eng., A 488 (1) (2008) 195–204.
[22] S.J. Dai, T. Xing, D.H. Wen, J.L. Yuan, Y. Dai, China Mech. Eng. 17 (10) (2006) 1007–1009.